EUROPEAN ORGANIZATION FOR NUCLEAR RESEARCH (CERN)

CERN-EP-2024-337
LHCb-PAPER-2024-049
January 22, 2025

Observation of the $\Lambda_b^0 \to J/\psi \Xi^- K^+$ and $\Xi_b^0 \to J/\psi \Xi^- \pi^+$ decays

LHCb collaboration[†]

Abstract

The first observation of the $\Xi_b^0 \to J/\psi \Xi^- \pi^+$ decay and the most precise measurement of the branching fraction of the $\Lambda_b^0 \to J/\psi \Xi^- K^+$ decay are reported, using proton-proton collision data from the LHCb experiment collected in 2016–2018 at a centre-of-mass energy of 13 TeV, corresponding to an integrated luminosity of $5.4\,\text{fb}^{-1}$. Using the $\Lambda_b^0 \to J/\psi \Lambda$ and $\Xi_b^- \to J/\psi \Xi^-$ decays as normalisation channels, the ratios of branching fractions are measured to be

$$\frac{\mathcal{B}(\Lambda_b^0 \to J/\psi \Xi^- K^+)}{\mathcal{B}(\Lambda_b^0 \to J/\psi \Lambda)} = (1.17 \pm 0.14 \pm 0.08) \times 10^{-2}\,,$$

$$\frac{\mathcal{B}(\Xi_b^0 \to J/\psi \Xi^- \pi^+)}{\mathcal{B}(\Xi_b^- \to J/\psi \Xi^-)} = (11.9 \pm 1.4 \pm 0.6) \times 10^{-2}\,,$$

where the first uncertainty is statistical and the second systematic.

Submitted to Eur. Phys. J. C

[†]Authors are listed at the end of this paper.

1 Introduction

The existence of pentaquark states has been predicted since the establishment of the quark model [1]. In 2015 the first pentaquark states were observed by the LHCb experiment in the spectrum of $\Lambda_b^0 \to J/\psi p K^-$ decays [2].[1] This observation sparked significant interest in the community, leading to various interpretations on the internal structure of these states [3–7]. In the subsequent years, numerous pentaquark states have been discovered in b-hadron decays to final states containing charmonium [8–11]. After the observation of pentaquarks with strangeness $S = 0$ and $S = 1$ in the $J/\psi p$ and $J/\psi \Lambda$ systems, the search for a pentaquark with $S = -2$ in the $J/\psi \Xi^-$ system is the next natural step [12,13]. In this paper, the foundation for these searches is laid by the observation of the $\Lambda_b^0 \to J/\psi \Xi^- K^+$ and $\Xi_b^0 \to J/\psi \Xi^- \pi^+$ decays.

Besides the search for exotic states in decay products including a charmonium resonance, the studied decay channels give insights into the dynamics of baryon-meson systems with one or two units of strangeness [14]. Of particular interest are $\overline{K}N$ meson-baryon interactions which are used to describe the $\Lambda(1405)$ resonance using Unitarised Chiral Perturbation Theory [15]. These interactions have been studied using data from $K^-p \to KN, \pi\Sigma, \pi^0\Lambda$ inelastic scattering, near threshold production of the $\Lambda(1405)$ resonance [16]. Scattering studies at higher energies — above the $K\Xi$ threshold — are interesting since they are sensitive to next-to-leading order terms of the Chiral Lagrangian [16]. Most of the $\overline{K}N \to K\Xi$ data come from antikaon-proton scattering, which includes both isospin $I = 0$ and $I = 1$ contributions. In contrast, K^-p scattering, which occurs in the decay process $\Lambda_b^0 \to J/\psi \Xi^- K^+$, and is restricted to $I = 0$ contribution in order to preserve the overall isospin of the decay. Studying this weak process therefore allows the $I = 0$ component to be isolated, thus enhancing our understanding of meson-baryon interactions [17]. In the $\Lambda_b^0 \to J/\psi \Xi^- K^+$ decay, the direct production of the $\Xi^- K^+$ final state is forbidden in the quark model, and is only reached via a two-step process, as shown in Fig. 1. First, the $\Lambda_b^0 \to J/\psi\{\Lambda\eta, pK^-, n\overline{K}\}$ decay proceeds via the weak interaction. Second, the meson-baryon pair produced in the decay scatters into a $\Xi^- K^+$ pair [16]. A measurement of the $m(\Xi^- K^+)$ spectrum in the $\Lambda_b^0 \to J/\psi \Xi^- K^+$ decay isolates the $I = 0$

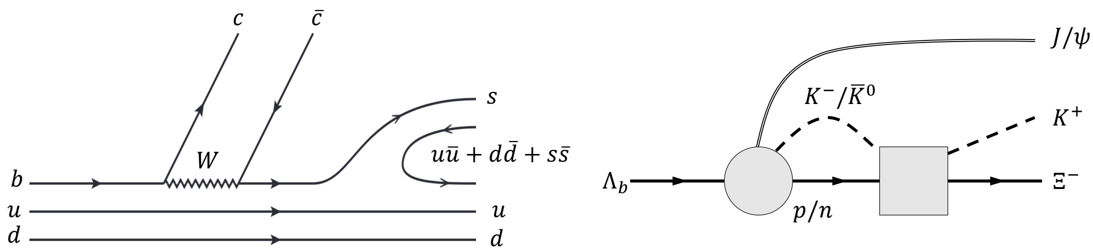

Figure 1: (Left) Production of a pK^-, $n\overline{K}^0$ or $\Lambda\eta$ pair from the weak decay $\Lambda_b^0 \to J/\psi\Lambda$ via a hadronisation mechanism. (Right) Final-state interaction of the meson-baryon pair, where the double line denotes the J/ψ meson, solid lines represent baryons and dashed lines denote the pseudoscalar mesons. The shaded circle and square stand for the production mechanism of the $J/\psi pK^-$ or $J/\psi n\overline{K}^0$, and the meson-baryon scattering matrix, respectively.

[1] Charge conjugation is implied throughout this paper.

contribution, and allows the $I = 0$ and $I = 1$ contributions in previous data [16] to be disentangled. As a consequence, the modelling of meson-baryon interaction above the $\Lambda(1405)$ resonance can be improved.

The $\Xi_b^0 \to J/\psi \Xi^- \pi^+$ decay has not yet been observed. This decay is expected to receive contributions from $\Xi_b^0 \to J/\psi \Xi^*(\Xi^- \pi^+)$ processes, where Ξ^* are excited states of the Ξ baryon. The first excitation of the Ξ baryon, the $\Xi(1530)^0$ state, is flavour-symmetric and would be suppressed in the $\Xi_b^0 \to \Xi(1530)^0$ transition due to the Ξ_b^0 state being flavour-antisymmetric [18]. Measuring the $\Xi_b^0 \to J/\psi \Xi(1530)^0$ decay rate is a method to quantify the mixing of symmetric and antisymmetric flavour states. The $\Xi^- \pi^+$ invariant-mass spectrum in $\Xi_b^0 \to J/\psi \Xi^- \pi^+$ decays can help explore possible mixing between flavour-symmetric and -antisymmetric contributions. Furthermore, the $\Xi_b^0 \to J/\psi \Xi^- \pi^+$ channel provides an excellent opportunity to search for charmonium pentaquark states. The first step towards the study of the decay dynamics is to observe these decay channels and analyse their mass spectra. This paper details the first measurement of the $\Xi_b^0 \to J/\psi \Xi^- \pi^+$ branching fraction and improves the precision of the $\Lambda_b^0 \to J/\psi \Xi^- K^+$ branching fraction with respect to the latest measurement by the CMS collaboration [19]. The measurements reported in this paper use pp collision data collected by the LHCb experiment in 2016–2018 at a centre-of-mass energy of 13 TeV, corresponding to an integrated luminosity of 5.4 fb^{-1}.

The $\Lambda_b^0 \to J/\psi \Xi^- K^+$ and $\Xi_b^0 \to J/\psi \Xi^- \pi^+$ signal channels are reconstructed through the $J/\psi \to \mu^+ \mu^-$, $\Xi^- \to \Lambda \pi^-$ and $\Lambda \to p \pi^-$ decays. The $\Lambda_b^0 \to J/\psi \Lambda$ and $\Xi_b^- \to J/\psi \Xi^-$ decay modes are used as normalisation channels due to their similar experimental signature. The choice of normalisation channels enable the cancellation of the dependence on b-hadron production rates and minimises systematic uncertainties related to final-state particle reconstruction. The ratios of branching fractions are measured as

$$\frac{\mathcal{B}(\Lambda_b^0 \to J/\psi \Xi^- K^+)}{\mathcal{B}(\Lambda_b^0 \to J/\psi \Lambda)} = \frac{N(\Lambda_b^0 \to J/\psi \Xi^- K^+)}{N(\Lambda_b^0 \to J/\psi \Lambda)} \cdot \frac{\varepsilon(\Lambda_b^0 \to J/\psi \Lambda)}{\varepsilon(\Lambda_b^0 \to J/\psi \Xi^- K^+)} \cdot \mathcal{B}(\Xi^- \to \Lambda \pi^-)\,, \quad (1)$$

$$\frac{\mathcal{B}(\Xi_b^0 \to J/\psi \Xi^- \pi^+)}{\mathcal{B}(\Xi_b^- \to J/\psi \Xi^-)} = \frac{N(\Xi_b^0 \to J/\psi \Xi^- \pi^+)}{N(\Xi_b^- \to J/\psi \Xi^-)} \cdot \frac{\varepsilon(\Xi_b^- \to J/\psi \Xi^-)}{\varepsilon(\Xi_b^0 \to J/\psi \Xi^- \pi^+)}\,, \quad (2)$$

where $\mathcal{B}$ is the branching fraction, N is the number of observed decays and ε is the total efficiency for the corresponding decay. An event selection is developed using simulated samples to optimise the search sensitivity. Correct estimation of the efficiencies relies on the accurate modelling of the physics processes and detector response in the simulation. The normalisation channels are used to correct for inaccuracies in the simulation for observables with a significant disagreement between simulation and data. After the selection is completed, the signal and normalisation yields are obtained from fits to the invariant-mass distributions of candidates in the selected data. In addition, the background-subtracted invariant-mass distributions of the $\Xi^- K^+$, $J/\psi K^+$ and $J/\psi \Xi^-$ pairs for the $\Lambda_b^0 \to J/\psi \Xi^- K^+$ channel, and the $\Xi^- \pi^+$, $J/\psi \pi^+$ and $J/\psi \Xi^-$ pairs for the $\Xi_b^0 \to J/\psi \Xi^- \pi^+$ channel are investigated. The background-subtracted samples are obtained using the `sPlot` technique [20, 21]. The invariant-mass signal regions were not examined until the full procedure had been finalised.

2 Detector and simulation

The LHCb detector [22, 23] is a single-arm forward spectrometer covering the pseudorapidity range $2 < \eta < 5$, designed for the study of particles containing b or c quarks. The detector used to to collect data in 2015–2018 (Run 2) includes a high-precision tracking system consisting of a silicon-strip vertex detector (VELO) surrounding the pp interaction region, a large-area silicon-strip detector, the Tracker Turicensis (TT), located upstream of a dipole magnet with a bending power of about $4\,\mathrm{T\,m}$, and three stations of silicon-strip detectors, straw drift tubes (T-stations) placed downstream of the magnet. The tracking system provides a measurement of the momentum, p, of charged particles with a relative uncertainty that varies from 0.5% at low momentum to 1.0% at $200\,\mathrm{GeV}/c$. The minimum distance of a track to a primary pp collision vertex (PV), the impact parameter (IP), is measured with a resolution of $(15 + 29/p_{\mathrm{T}})\,\mu\mathrm{m}$, where p_{T} is the component of the momentum transverse to the beam, in GeV/c. Different types of charged hadrons are distinguished using information from two ring-imaging Cherenkov detectors. Muons are identified by a system composed of alternating layers of iron and multiwire proportional chambers. The online event selection [24] is performed by a trigger which consists of a hardware stage, based on information from the calorimeter and muon systems, followed by two software stages, which apply a partial and full event reconstruction, respectively. At the hardware trigger stage, events are required to have muon or dimuon candidates with high p_{T}. The software trigger requires a two-track secondary vertex with a significant displacement from any PV. At least one charged particle must have $p_{\mathrm{T}} > 1.6\,\mathrm{GeV}/c$ and be inconsistent with originating from a PV.

Simulated samples are used to develop the selection strategy, compute the efficiencies and model the shape of the invariant-mass distribution of the signal decays. In the simulation, pp collisions are generated using PYTHIA [25] with a specific LHCb configuration [26]. Decays of unstable particles are described by EVTGEN [27], in which final-state radiation is generated using PHOTOS [28]. The interaction of the generated particles with the detector, and its response, are implemented using the GEANT4 toolkit [29] as described in Ref. [30]. For each generated signal decay the underlying pp interaction is reused multiple times [31].

3 Candidate selection and efficiencies

The selection begins by identifying well-reconstructed tracks that do not originate from any PV. Candidates with two oppositely charged tracks identified as muons are selected. Each muon candidate must fulfil $p_{\mathrm{T}} > 250\,\mathrm{MeV}/c$ requirement. Dimuon pairs that form a good-quality vertex significantly displaced from any PV are combined to form J/ψ candidates. The dimuon pair must have a reconstructed invariant mass compatible with the nominal mass of the J/ψ meson. Oppositely charged tracks assigned to proton and pion mass hypotheses are combined to form Λ candidates. The $p\pi^-$ invariant mass is required to be within $\pm10\,\mathrm{MeV}/c^2$ of the known Λ mass [32]. The Λ candidates are further combined with another particle, assigned the pion mass hypothesis, to reconstruct Ξ^- candidates. The selected $\Lambda\pi^-$ pairs must have a p_{T} larger than $250\,\mathrm{MeV}/c^2$ and an invariant mass within $\pm20\,\mathrm{MeV}/c^2$ of the known Ξ^- mass [32]. For reference, the mass resolution of the Λ and Ξ^- signals are about $1.7\,\mathrm{MeV}/c^2$ and $3.0\,\mathrm{MeV}/c^2$, respectively.

Given the relatively large lifetime of the Λ and Ξ^- baryons, most of these candidates decay downstream of the VELO, but before reaching the TT. Tracks that are reconstructed only from hits in the TT and the T-stations are called downstream tracks. Tracks that are reconstructed using hits in the VELO, the T-stations, and optionally in the TT, are called long tracks. Long tracks profit from the superior resolution of the vertex detector and have better mass, momentum and vertex position resolution than downstream tracks. The considered $\Lambda \to p\pi^-$ candidates can be reconstructed from two long tracks or two downstream tracks. Similarly, the $\Xi^- \to \Lambda\pi^-$ decay is reconstructed using three main categories of track-type combinations: (i) both Λ and π^- candidates reconstructed only from long tracks, (ii) both Λ and π^- candidates reconstructed only from downstream tracks, and (iii) the Λ candidate reconstructed from two downstream tracks and the accompanying π^- candidate reconstructed as a long track. The Λ_b^0 (Ξ_b^0) signal candidate is formed by combining the J/ψ and Ξ^- candidates with a long track identified as a K^+ (π^+) candidate with $p_{\mathrm{T}} > 250\,\mathrm{MeV}/c$. Similarly, J/ψ and Λ (Ξ^-) candidates are combined to form Λ_b^0 (Ξ_b^-) candidates corresponding to the normalisation channel decay. Both Λ and Ξ^- candidates are required to have a decay time greater than 2 ps to reject background from short-lived particles. The Λ_b^0 (Ξ_b) decay vertices must have a good fit quality and be significantly displaced from any PV. A kinematic fit [33] is performed to improve the b-hadron mass resolution by constraining the mass hypothesis of the J/ψ, Ξ^- and Λ candidates to their known masses [32] and requiring the b hadron to originate from its associated PV[2]. Candidates with a poor quality of the kinematic fit or a Λ_b^0 (Ξ_b) invariant mass from the kinematic fit outside the range $[5360, 5900]$ ($[5700, 6100]$) MeV/c^2 are rejected.

The final step of the selection for the four decays channels is to apply a boosted decision tree (BDT) [34,35] classifier implemented using the XGBoost toolkit [36]. Each classifier is trained to distinguish between the specific b-hadron decay and combinatorial background. Simulation samples are used as a proxy for the specific b-hadron decays. The background samples are taken from the high invariant-mass sideband [5700, 5900] ([5900, 6100]) MeV/c^2 of selected Λ_b^0 (Ξ_b) data candidates. The BDT classifier exploits the discriminating power of the IP of the π^- meson from the Ξ^- decay, and Λ decay products with respect to any PV; the difference in the vertex-fit χ^2 of a given PV reconstructed with and without the b-hadron and the muons; the χ^2 of the kinematic fit; the decay time of the b hadron and Ξ^- baryon; and the p_{T} of the Ξ^- candidate. Most of the training variables are common between the signal and normalisation channels, with the exception of variables associated with the Ξ^- candidate that are excluded when analysing the $\Lambda_b^0 \to J/\psi\Lambda$ mode. The BDT working point is chosen by maximising a figure of merit [37], defined as $\varepsilon_{\mathrm{s}}/(\sqrt{B} + 2.5)$, where ε_{s} is the efficiency of the requirement on the BDT output for simulated signal events, and B is the background yield in a region within 3 sigmas around the nominal b-hadron mass, extrapolated from the high invariant-mass sideband. The BDT classifier removes more than 99% of the background while retaining approximately 70% of the signal in the four considered decay modes. When more than one candidate is selected per event, the candidate with the highest BDT score is kept.

The total efficiency is calculated as the product of efficiencies of detector acceptance, reconstruction, and selection. Accurate simulation is crucial to determine such selection efficiencies, and also to train the BDT algorithms and model the signal mass shapes.

[2]The associated PV is defined as the PV that fits best to the flight direction of the b-hadron candidate.

Discrepancies between data and simulation are observed and corrected for in the b-baryon p_{T}, the χ^2 of the kinematic fit, angular and two-body invariant-mass distributions, and particle identification and tracking efficiencies. The corrections are derived sequentially, *i.e.* adjusting the distribution for one variable at a time. Potential correlations between variables are accounted for by deriving each correction factor on top of previous ones. The particle identification efficiencies for the different particle species are measured using charm hadron data samples reconstructed without the use of PID information [38]. The correction factors for the tracking efficiencies are derived from a dedicated data sample of $J/\psi \to \mu^+\mu^-$ decays [39]. The correction factors for b-baryon p_{T} and the χ^2 of the kinematic fit are extracted from a comparison of $\Lambda_b^0 \to J/\psi\Lambda$ and $\Xi_b^- \to J/\psi\Xi^-$ decays between background-subtracted data and simulated samples and applied to both signal and normalisation channels. The angular distribution could differ between the signal and normalisation channels, and thus the above correction factors are derived independently for each of the four channels. The decay dynamics of the signal channels are also corrected for the $m(J/\psi\Xi^-)$ and $m(\Xi^-K^+)$, or $m(\Xi^-\pi^+)$, distributions. The variables corrected are those that demonstrated a significant correlation with the efficiency. These correction factors are derived from the $\Lambda_b^0 \to J/\psi\Xi^-K^+$ and $\Xi_b^0 \to J/\psi\Xi^-\pi^+$ signal channels No significant correlation is observed between the discriminant variable used for the background-subtraction method, the b-hadron invariant mass improved by the kinematic fit, and the corrected variables. The ratios of efficiencies between the Λ_b^0 and Ξ_b modes, required in Eqs. 1 and 2, are determined to be

$$\frac{\varepsilon(\Lambda_b^0 \to J/\psi\Lambda)}{\varepsilon(\Lambda_b^0 \to J/\psi\Xi^-K^+)} = 5.30 \pm 0.05\,,$$
$$\frac{\varepsilon(\Xi_b^- \to J/\psi\Xi^-)}{\varepsilon(\Xi_b^0 \to J/\psi\Xi^-\pi^+)} = 1.64 \pm 0.02\,,$$

where the uncertainty is due to the limited size of the simulation samples. This uncertainty is propagated to the branching fraction ratios as a source of systematic uncertainty in Sec. 5.

4 Signal yield determination

An extended unbinned maximum-likelihood fit is performed to the b-hadron invariant-mass spectrum of the $\Lambda_b^0 \to J/\psi\Xi^-K^+$ and $\Lambda_b^0 \to J/\psi\Lambda$ modes in the range [5360, 5900] MeV/c^2. An analogous, independent fit is performed to the $\Xi_b^0 \to J/\psi\Xi^-\pi^+$ and $\Xi_b^- \to J/\psi\Xi^-$ candidates in the range [5700, 6100] MeV/c^2. The invariant-mass shape of the $\Lambda_b^0 \to J/\psi\Lambda$ decay mode is modelled by a Hypatia function [40]. The signal for the other three channels is modelled by the sum of two Crystal Ball functions [41] with common mean and width. The tail parameters for both signal models, Hypatia and two Crystal Ball functions, are fixed according to simulation. The shape of the invariant-mass distribution of the combinatorial background is modelled by an exponential function with a slope varying freely in the fit. Non-negligible contribution of physical backgrounds is only observed in the $\Lambda_b^0 \to J/\psi\Lambda$ channel at the level of about 20%. The two main background sources are $B^0 \to J/\psi K_{\mathrm{S}}^0$ and $\Xi_b^- \to J/\psi\Xi^-$ decays. The $B^0 \to J/\psi K_{\mathrm{S}}^0$ decay can be misidentified as a $\Lambda_b^0 \to J/\psi\Lambda$ candidate if the proton hypothesis is wrongly assigned to the π^+ meson in the K_{S}^0 decay. Additionally, missing the pion from the $\Xi^- \to \Lambda\pi^-$ decay leads to a $\Xi_b^- \to J/\psi\Xi^-$ decay

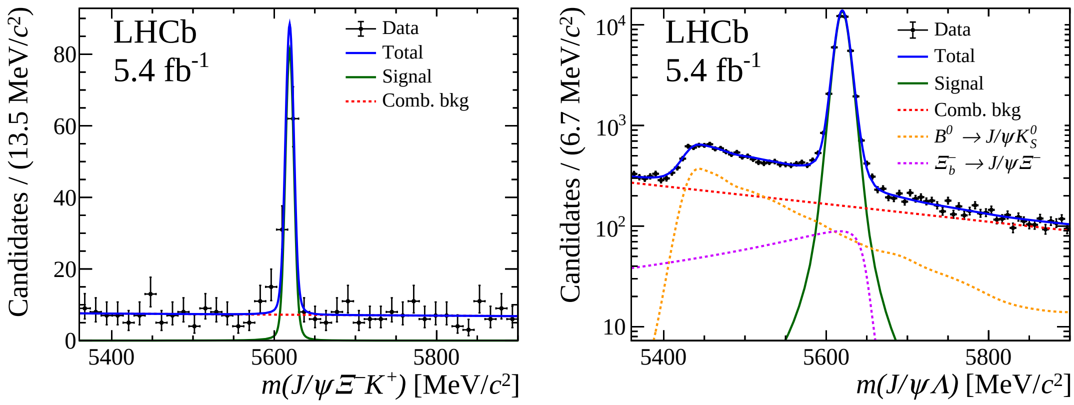

Figure 2: Invariant-mass distribution of selected (left) $\Lambda_b^0 \to J/\psi \Xi^- K^+$ and (right) $\Lambda_b^0 \to J/\psi \Lambda$ candidates with the result of the fit also shown.

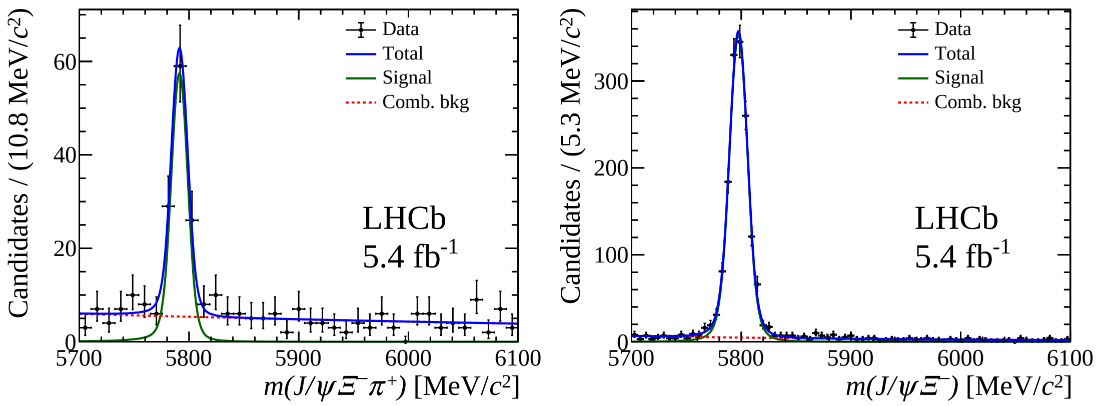

Figure 3: Invariant-mass distribution of selected (left) $\Xi_b^0 \to J/\psi \Xi^- \pi^+$ and (right) $\Xi_b^- \to J/\psi \Xi^-$ candidates with the result of the fit also shown.

that is partially reconstructed as a $\Lambda_b^0 \to J/\psi \Lambda$ candidate. The invariant-mass shapes of the misidentified $B^0 \to J/\psi K^0_S$ and partially reconstructed $\Xi_b^- \to J/\psi \Xi^-$ backgrounds are derived from simulation in terms of a nonparametric probability density function using a kernel density estimation method [42, 43] and a Johnson S_U function [44], respectively. The shapes of these functions are fixed from simulation.

Figures 2 and 3 show the result of the fits to the invariant-mass spectra for Λ_b^0 and Ξ_b candidates, respectively. The Λ_b^0 invariant-mass fits determine yields of 84 ± 10 $\Lambda_b^0 \to J/\psi \Xi^- K^+$ signal and 39390 ± 220 $\Lambda_b^0 \to J/\psi \Lambda$ normalisation decays. The Ξ_b invariant-mass fits determine yields of 107 ± 12 $\Xi_b^0 \to J/\psi \Xi^- \pi^+$ signal and 1450 ± 40 $\Xi_b^- \to J/\psi \Xi^-$ normalisation decays. Both signal modes are observed with a significance greater than 10σ using the Wilk's theorem [45].

5 Systematic uncertainties

Systematic uncertainties on the $\mathcal{B}(\Lambda_b^0 \to J/\psi \Xi^- K^+)/\mathcal{B}(\Lambda_b^0 \to J/\psi \Lambda)$ and $\mathcal{B}(\Xi_b^0 \to J/\psi \Xi^- \pi^+)/\mathcal{B}(\Xi_b^- \to J/\psi \Xi^-)$ measurements arise from several sources. A summary of the uncertainties is provided in Table 1.

Table 1: Summary of relative systematic uncertainties (in percent) for the measured ratio of branching fractions. The individual sources are described in the text. The total relative uncertainty is determined by adding the individual sources in quadrature.

Source	$\frac{\mathcal{B}(\Lambda_b^0 \to J/\psi \Xi^- K^+)}{\mathcal{B}(\Lambda_b^0 \to J/\psi \Lambda)}$ [%]	$\frac{\mathcal{B}(\Xi_b^0 \to J/\psi \Xi^- \pi^+)}{\mathcal{B}(\Xi_b^- \to J/\psi \Xi^-)}$ [%]
Fit model	1.9	1.3
Size of the simulated samples	0.9	1.2
Corrections to simulation	3.4	1.1
Alternative corrections	1.1	1.2
Additional corrections	1.9	1.0
Tracking efficiency	1.5	1.4
Truth matching	1.3	1.2
Phase-space model	4.5	3.8
Total	6.7	5.0

The systematic effect due to the choice of the invariant-mass fit model is assessed by means of pseudoexperiments wherein the invariant-mass distribution is generated with an alternative model and fitted using the baseline model. The alternative model replaces the two Crystal Ball functions by an Hypatia function (or vice versa for the $\Lambda_b^0 \to J/\psi \Lambda$ case) for the signal. The physical backgrounds in the $\Lambda_b^0 \to J/\psi \Lambda$ channel are both modelled with a single Crystal Ball function in the alternative model.

The uncertainty on the selection efficiencies originating from the limited size of the simulated samples is propagated to the branching fraction and considered as a systematic uncertainty.

The corrections applied to the simulation to improve the agreement with data are obtained with an uncertainty. The effect of this limited precision is assessed by varying the corrections within their uncertainty and recomputing the efficiencies 100 times. The standard deviation of the efficiency variation is assigned as a systematic uncertainty.

The χ^2 distribution of each kinematic fit is corrected using the normalisation channels as calibration samples. While the normalisation decay topology is similar, it is not identical to the signal decay. Alternative corrections for the simulations are derived by swapping the calibration channel, *i.e.* using the $\Lambda_b^0 \to J/\psi \Lambda$ channel for $\Xi_b^0 \to J/\psi \Xi^- \pi^+$ corrections and the $\Xi_b^- \to J/\psi \Xi^-$ channel for $\Lambda_b^0 \to J/\psi \Xi^- K^+$ corrections. The variation in the efficiency is assigned as the systematic uncertainty.

After applying the baseline corrections to the simulation, some level of mismodelling remains in variables not used directly in the selection. The effect of this mismodelling is assessed by recomputing the efficiencies after correcting the additional distributions and the difference with respect to the baseline efficiency is added as a systematic uncertainty.

The signal channels feature a prompt hadron without a counterpart in the normalisation channel. An additional uncertainty on tracking efficiency of 1.4% for pions and 1.1% for kaons is added which accounts for hadronic interactions that do not cancel in the efficiency ratio. Additionally, the pion from the $\Xi^- \to \Lambda \pi^-$ decay in the $\Lambda_b^0 \to J/\psi \Xi^- K^+$ signal channel does not have a counterpart in the $\Lambda_b^0 \to J/\psi \Lambda$ normalisation channel. This pion can be reconstructed as a downstream track, whose reconstruction efficiency is controlled only at the 1% level [46]. The 1% precision is also added as systematic uncertainty to the Λ_b^0 result.

Efficiencies are determined from simulated samples and rely on an accurate match between generated and reconstructed decays. In some cases, this so-called truth matching can fail if the fraction of hits associated between the reconstructed track and the generated particle does not reach a minimum threshold. The effect of such potential incorrect matching is evaluated by recomputing the efficiencies with an alternative method that does not rely on truth matching. Instead, the number of signal events after the selection, required to compute the efficiency, is determined by an invariant-mass fit of the b-hadron spectrum, similar to the approach used for data. The difference in efficiency derived from the baseline and the alternative method is assigned as the systematic uncertainty.

Lastly, inaccuracies in the phase-space model used for signal simulation could affect the derived efficiency. The decay dynamics and angular distributions are corrected using the signal channels. The effect of the limited precision on the derived corrections is assessed by recalculating 100 times the efficiencies after varying the correction factors within their statistical uncertainty. The standard deviation is assigned as the systematic uncertainty.

The systematic uncertainties described in the section above are considered to be uncorrelated and added in quadrature.

6 Results

By combining the signal and normalisation yields from the invariant-mass fits with the selection efficiency ratios as shown in Eqs. 1 and 2, and using the known branching fraction $\mathcal{B}(\Xi^- \to \Lambda\pi^-) = 0.99887 \pm 0.00035$ [32], the following results are obtained:

$$\frac{\mathcal{B}(\Lambda_b^0 \to J/\psi \Xi^- K^+)}{\mathcal{B}(\Lambda_b^0 \to J/\psi \Lambda)} = (1.17 \pm 0.14 \pm 0.08) \times 10^{-2}\,,$$
$$\frac{\mathcal{B}(\Xi_b^0 \to J/\psi \Xi^- \pi^+)}{\mathcal{B}(\Xi_b^- \to J/\psi \Xi^-)} = (11.9 \pm 1.4 \pm 0.6) \times 10^{-2}\,,$$

where the first uncertainty is statistical, and the second is systematic. It is possible to convert the $\mathcal{B}(\Lambda_b^0 \to J/\psi \Xi^- K^+)/\mathcal{B}(\Lambda_b^0 \to J/\psi \Lambda)$ ratio to the $\mathcal{B}(\Lambda_b^0 \to J/\psi \Xi^- K^+)/\mathcal{B}(\Lambda_b^0 \to \psi(2S)\Lambda)$ ratio using the world average of $\mathcal{B}(\Lambda_b^0 \to \psi(2S)\Lambda)/\mathcal{B}(\Lambda_b^0 \to J/\psi \Lambda) = 0.508 \pm 0.023$ [32] and compare it with the CMS result [19]:

$$\left.\frac{\mathcal{B}(\Lambda_b^0 \to J/\psi \Xi^- K^+)}{\mathcal{B}(\Lambda_b^0 \to \psi(2S)\Lambda)}\right|_{\text{CMS}} = (3.4 \pm 1.2) \times 10^{-2}\,,$$
$$\left.\frac{\mathcal{B}(\Lambda_b^0 \to J/\psi \Xi^- K^+)}{\mathcal{B}(\Lambda_b^0 \to \psi(2S)\Lambda)}\right|_{\text{LHCb}} = (2.3 \pm 0.3) \times 10^{-2}\,.$$

The LHCb result reported in this paper is compatible with the one obtained by CMS and improves the precision by a factor of 4.

The branching fraction of the signal channels is obtained from the measured ratios using the known branching fractions of the normalisation channels. The values $\mathcal{B}(\Lambda_b^0 \to J/\psi \Lambda) = (3.36 \pm 1.11) \times 10^{-4}$ and $\mathcal{B}(\Xi_b^- \to J/\psi \Xi^-) = (5.4 \pm 2.4) \times 10^{-4}$ from

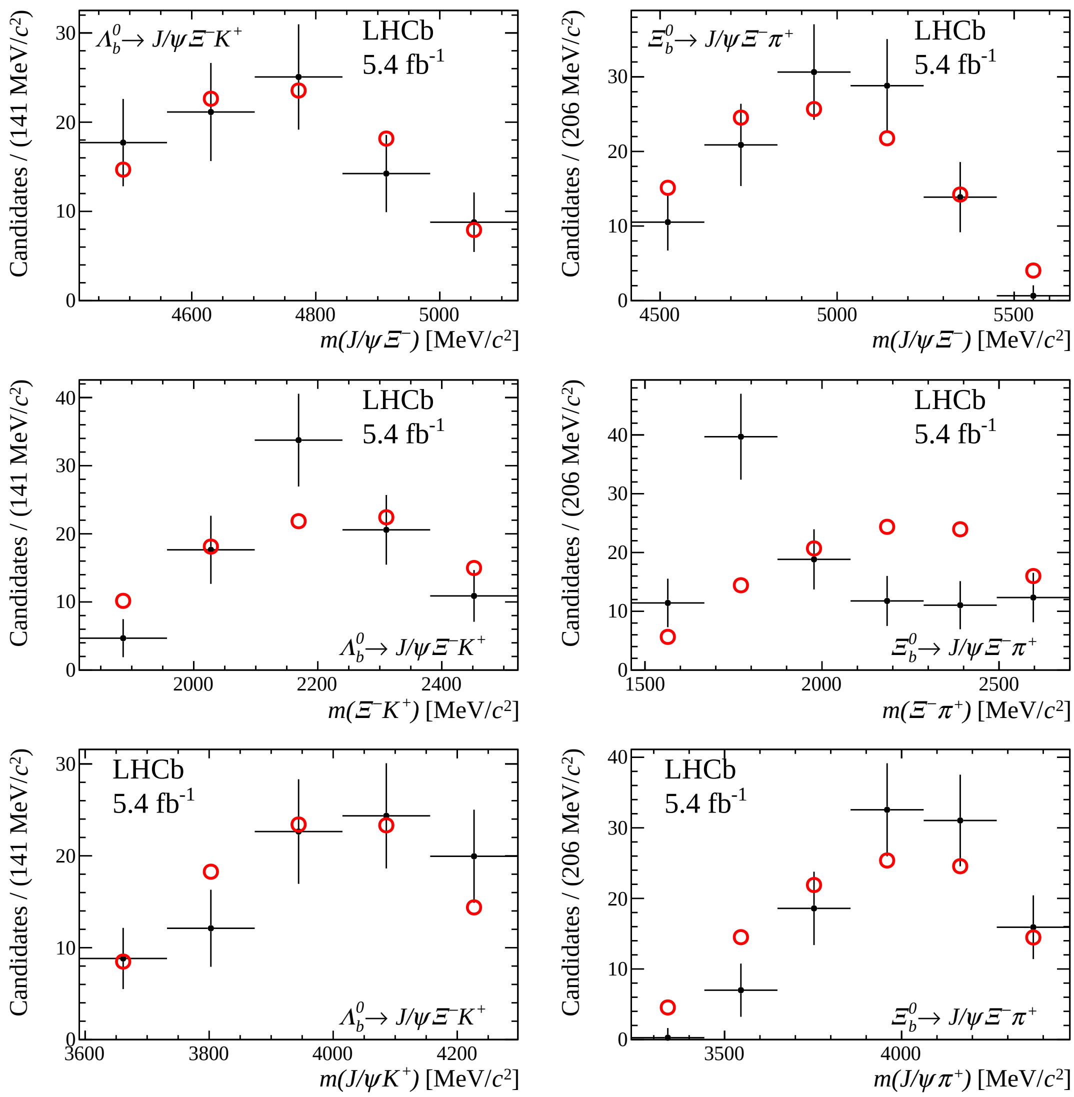

Figure 4: Invariant-mass distribution of the (top) $J/\psi\Xi^-$, (centre) Ξ^-K^+ or $\Xi^-\pi^+$ and (bottom) $J/\psi K^+$ or $J/\psi\pi^+$ systems for the (left) $\Lambda_b^0 \to J/\psi\Xi^-K^+$ and (right) $\Xi_b^0 \to J/\psi\Xi^-\pi^+$ decays. The (black) background-subtracted data is compared to the (red) phase-space simulation including all weights except those for the helicity angles and two-body invariant-mass variables.

Ref. [47] are used. The signal branching fractions are determined to be:

$$\mathcal{B}(\Lambda_b^0 \to J/\psi\Xi^-K^+) = (3.93 \pm 0.47 \pm 0.27 \pm 1.30) \times 10^{-6}\,,$$
$$\mathcal{B}(\Xi_b^0 \to J/\psi\Xi^-\pi^+) = (6.42 \pm 0.76 \pm 0.32 \pm 2.86) \times 10^{-5}\,,$$

where the first uncertainty is statistical, the second is systematic and the third is due to the external value of the normalisation branching fraction.

The background-subtracted distributions of $m(J/\psi\Xi^-)$, $m(\Xi^-K^+)$ and $m(\Xi^-\pi^+)$ are shown in Fig. 4 and are compared with the phase-space simulation. From this comparison, the only data-simulation disagreement that could point towards a resonance appears in the $m(\Xi^-\pi^+)$ range $[1670, 1850]$ MeV/c^2 for $\Xi_b^0 \to J/\psi\Xi^-\pi^+$ candidates. Two resonances, $\Xi(1690)$ and $\Xi(1820)$, with invariant-mass in this range are found in the literature. While the $\Xi(1690)$ resonance is observed to mainly decay to $\Xi^-\pi^+$, the $\Xi(1820)$ resonance is expected to primarily decay to $\Lambda\overline{K}$. Consequently, the decay channel $\Xi_b^0 \to J/\psi \Xi^- \pi^+$ is more likely to receive contributions from the $\Xi_b^0 \to J/\psi \Xi(1690)$ transition. However, no significant evidence supporting this hypothesis is observed in the current measurement. Larger data samples are needed to perform a quantitative study, which is left for the future.

7 Conclusions

In summary, a sample of pp collision data corresponding to an integrated luminosity of $5.4\,\text{fb}^{-1}$ is used to measure the $\mathcal{B}(\Lambda_b^0 \to J/\psi \Xi^- K^+)/\mathcal{B}(\Lambda_b^0 \to J/\psi \Lambda)$ and $\mathcal{B}(\Xi_b^0 \to J/\psi \Xi^- \pi^+)/\mathcal{B}(\Xi_b^- \to J/\psi \Xi^-)$ ratios. The $\mathcal{B}(\Lambda_b^0 \to J/\psi \Xi^- K^+)/\mathcal{B}(\Lambda_b^0 \to J/\psi \Lambda)$ result is compatible with the CMS measurement and improves its precision by a factor of four. The $\Xi_b^0 \to J/\psi \Xi^- \pi^+$ decay is observed for the first time. The branching fraction of the $\Lambda_b^0 \to J/\psi \Xi^- K^+$ and $\Xi_b^0 \to J/\psi \Xi^- \pi^+$ decays are measured using the known branching fraction of the normalisation channels. This analysis paves the way for future amplitude analysis using larger data sets that will be collected by the upgraded LHCb experiment.

Acknowledgements

We express our gratitude to our colleagues in the CERN accelerator departments for the excellent performance of the LHC. We thank the technical and administrative staff at the LHCb institutes. We acknowledge support from CERN and from the national agencies: ARC and ARDC (Australia); CAPES, CNPq, FAPERJ and FINEP (Brazil); MOST and NSFC (China); CNRS/IN2P3 (France); BMBF, DFG and MPG (Germany); INFN (Italy); NWO (Netherlands); MNiSW and NCN (Poland); MCID/IFA (Romania); MICIU and AEI (Spain); SNSF and SER (Switzerland); NASU (Ukraine); STFC (United Kingdom); DOE NP and NSF (USA). We acknowledge the computing resources that are provided by CERN, IN2P3 (France), KIT and DESY (Germany), INFN (Italy), SURF (Netherlands), PIC (Spain), GridPP (United Kingdom), CSCS (Switzerland), IFIN-HH (Romania), CBPF (Brazil), and Polish WLCG (Poland). We are indebted to the communities behind the multiple open-source software packages on which we depend. Individual groups or members have received support from Key Research Program of Frontier Sciences of CAS, CAS PIFI, CAS CCEPP, Fundamental Research Funds for the Central Universities, and Sci. & Tech. Program of Guangzhou (China); Minciencias (Colombia); EPLANET, Marie Skłodowska-Curie Actions, ERC and NextGenerationEU (European Union); A*MIDEX, ANR, IPhU and Labex P2IO, and Région Auvergne-Rhône-Alpes (France); AvH Foundation (Germany); ICSC (Italy); Severo Ochoa and María de Maeztu Units of Excellence, GVA, XuntaGal, GENCAT, InTalent-Inditex and Prog. Atracción Talento CM (Spain); SRC (Sweden); the Leverhulme Trust, the Royal Society and UKRI (United Kingdom).

References

[1] M. Gell-Mann, *A schematic model of baryons and mesons*, Phys. Lett. **8** (1964) 214; G. Zweig, *An SU_3 model for strong interaction symmetry and its breaking; Version 1* CERN-TH-401, CERN, Geneva, 1964.

[2] LHCb collaboration, R. Aaij *et al.*, *Observation of $J/\psi p$ resonances consistent with pentaquark states in $\Lambda_b^0 \to J/\psi p K^-$ decays*, Phys. Rev. Lett. **115** (2015) 072001, arXiv:1507.03414.

[3] M.-L. Du *et al.*, *Interpretation of the LHCb P_c states as hadronic molecules and hints of a narrow $P_c(4380)$*, Phys. Rev. Lett. **124** (2020) 072001, arXiv:1910.11846.

[4] L. Roca, J. Nieves, and E. Oset, *LHCb pentaquark as a $\bar{D}^*\Sigma_c - \bar{D}^*\Sigma_c^*$ molecular state*, Phys. Rev **D92** (2015) 094003, arXiv:1507.04249.

[5] S. X. Nakamura, *$P_c(4312)^+$, $P_c(4380)^+$, and $P_c(4457)^+$ as double triangle cusps*, Phys. Rev. **D103** (2021) 111503, arXiv:2103.06817.

[6] M. I. Eides, V. Y. Petrov, and M. V. Polyakov, *Pentaquarks with hidden charm as hadroquarkonia*, Eur. Phys. J. **C78** (2018) 36, arXiv:1709.09523.

[7] E. Santopinto and A. Giachino, *Compact pentaquark structures*, Phys. Rev **D96** (2017) 014014, arXiv:1604.03769.

[8] LHCb collaboration, R. Aaij *et al.*, *Observation of a narrow pentaquark state, $P_c(4312)^+$, and of two-peak structure of the $P_c(4450)^+$*, Phys. Rev. Lett. **122** (2019) 222001, arXiv:1904.03947.

[9] LHCb collaboration, R. Aaij *et al.*, *Evidence of a $J/\psi\Lambda$ structure and observation of excited Ξ^- states in the $\Xi_b^- \to J/\psi\Lambda K^-$ decay*, Science Bulletin **66** (2021) 1278, arXiv:2012.10380.

[10] LHCb collaboration, R. Aaij *et al.*, *Observation of a $J/\psi\Lambda$ resonance consistent with a strange pentaquark candidate in $B^- \to J/\psi\Lambda\overline{p}$ decays*, Phys. Rev. Lett. **131** (2023) 031901, arXiv:2210.10346.

[11] LHCb collaboration, R. Aaij *et al.*, *Evidence for a new structure in the $J/\psi p$ and $J/\psi\overline{p}$ systems in $B_s^0 \to J/\psi p\overline{p}$ decays*, Phys. Rev. Lett. **128** (2022) 062001, arXiv:2108.04720.

[12] F.-L. Wang, X.-D. Yang, R. Chen, and X. Liu, *Hidden-charm pentaquarks with triple strangeness due to the $\Omega_c^{(*)}\overline{D}_s^{(*)}$ interactions*, Phys. Rev. **D103** (2021) 054025, arXiv:2101.11200.

[13] K. Azizi, Y. Sarac, and H. Sundu, *Investigation of hidden-charm double strange pentaquark candidate P_{css} via its mass and strong decays*, Eur. Phys. J. **C82** (2022) 543, arXiv:2112.15543.

[14] J. A. Oller, *About meson-baryon scattering with strangeness −1*, in *9th International Conference on Hypernuclear and Strange Particle Physics*, 237–242, 2007.

[15] D. Cabrera, L. Tolos, J. Aichelin, and E. Bratkovskaya, *Strange meson-baryon interaction in hot and dense medium: recent progress for a road to GSI/FAIR*, J. Phys. Conf. Ser. **668** (2016) 012048, arXiv:1510.07265.

[16] A. Feijoo, V. K. Magas, A. Ramos, and E. Oset, *$\Lambda_b \to J/\psi\ K\ \Xi$ decay and the higher order chiral terms of the meson baryon interaction*, Phys. Rev **D92** (2015) 076015, Erratum ibid. **D95** (2017) 351, arXiv:1507.04640.

[17] L. Roca, M. Mai, E. Oset, and U.-G. Meißner, *Predictions for the $\Lambda_b \to J/\psi\ \Lambda(1405)$ decay*, Eur. Phys. J **C75** (2015) 218, arXiv:1503.02936.

[18] L. Oliver, J.-C. Raynal, and R. Sinha, *Note on new interesting baryon channels to measure the photon polarization in $b \to s\gamma$*, Phys. Rev. **D82** (2010) 117502, arXiv:1007.3632.

[19] CMS collaboration, A. Hayrapetyan *et al.*, *Observation of the $\Lambda_b^0 \to J/\psi \Xi^- K^+$ decay*, Eur. Phys. J **C84** (2024) 1062, arXiv:2401.16303.

[20] M. Pivk and F. R. Le Diberder, *sPlot: A statistical tool to unfold data distributions*, Nucl. Instrum. Meth. **A555** (2005) 356, arXiv:physics/0402083.

[21] H. Dembinski, M. Kenzie, C. Langenbruch, and M. Schmelling, *Custom Orthogonal Weight functions (COWs) for event classification*, Nucl. Instrum. Meth. **A1040** (2022) 167270, arXiv:2112.04574.

[22] LHCb collaboration, A. A. Alves Jr. *et al.*, *The LHCb detector at the LHC*, JINST **3** (2008) S08005.

[23] LHCb collaboration, R. Aaij *et al.*, *LHCb detector performance*, Int. J. Mod. Phys. **A30** (2015) 1530022, arXiv:1412.6352.

[24] R. Aaij *et al.*, *Design and performance of the LHCb trigger and full real-time reconstruction in Run 2 of the LHC*, JINST **14** (2019) P04013, arXiv:1812.10790.

[25] T. Sjöstrand, S. Mrenna, and P. Skands, *PYTHIA 6.4 physics and manual*, JHEP **05** (2006) 026, arXiv:hep-ph/0603175.

[26] I. Belyaev *et al.*, *Handling of the generation of primary events in Gauss, the LHCb simulation framework*, J. Phys. Conf. Ser. **331** (2011) 032047.

[27] D. J. Lange, *The EvtGen particle decay simulation package*, Nucl. Instrum. Meth. **A462** (2001) 152.

[28] N. Davidson, T. Przedzinski, and Z. Was, *PHOTOS interface in C++: Technical and physics documentation*, Comp. Phys. Comm. **199** (2016) 86, arXiv:1011.0937.

[29] Geant4 collaboration, J. Allison *et al.*, *Geant4 developments and applications*, IEEE Trans. Nucl. Sci. **53** (2006) 270; Geant4 collaboration, S. Agostinelli *et al.*, *Geant4: A simulation toolkit*, Nucl. Instrum. Meth. **A506** (2003) 250.

[30] M. Clemencic *et al.*, *The LHCb simulation application, Gauss: Design, evolution and experience*, J. Phys. Conf. Ser. **331** (2011) 032023.

[31] D. Müller, M. Clemencic, G. Corti, and M. Gersabeck, *ReDecay: A novel approach to speed up the simulation at LHCb*, Eur. Phys. J. **C78** (2018) 1009, arXiv:1810.10362.

[32] Particle Data Group, S. Navas *et al.*, *Review of particle physics*, Phys. Rev. **D110** (2024) 030001.

[33] W. D. Hulsbergen, *Decay chain fitting with a Kalman filter*, Nucl. Instrum. Meth. **A552** (2005) 566, arXiv:physics/0503191.

[34] L. Breiman, J. H. Friedman, R. A. Olshen, and C. J. Stone, *Classification and regression trees*, Wadsworth international group, Belmont, California, USA, 1984.

[35] Y. Freund and R. E. Schapire, *A decision-theoretic generalization of on-line learning and an application to boosting*, J. Comput. Syst. Sci. **55** (1997) 119.

[36] T. Chen and C. Guestrin, *XGBoost: A scalable tree boosting system*, doi: 10.1145/2939672.2939785 arXiv:1603.02754.

[37] G. Punzi, *Sensitivity of searches for new signals and its optimization*, eConf **C030908** (2003) MODT002, arXiv:physics/0308063.

[38] R. Aaij *et al.*, *Selection and processing of calibration samples to measure the particle identification performance of the LHCb experiment in Run 2*, Eur. Phys. J. Tech. Instr. **6** (2019) 1, arXiv:1803.00824.

[39] LHCb collaboration, R. Aaij *et al.*, *Measurement of the track reconstruction efficiency at LHCb*, JINST **10** (2015) P02007, arXiv:1408.1251.

[40] D. Martínez Santos and F. Dupertuis, *Mass distributions marginalized over per-event errors*, Nucl. Instrum. Meth. **A764** (2014) 150, arXiv:1312.5000.

[41] T. Skwarnicki, *A study of the radiative cascade transitions between the Upsilon-prime and Upsilon resonances*, PhD thesis, Institute of Nuclear Physics, Krakow, 1986, DESY-F31-86-02.

[42] W. Verkerke and D. P. Kirkby, *The RooFit toolkit for data modeling*, eConf **C0303241** (2003) MOLT007, arXiv:physics/0306116.

[43] K. Cranmer, *Kernel estimation in high-energy physics*, Computer Physics Communications **136** (2001) 198.

[44] N. L. Johnson, *Systems of frequency curves generated by methods of translation*, Biometrika **36** (1949) 149.

[45] S. S. Wilks, *The large-sample distribution of the likelihood ratio for testing composite hypotheses*, Ann. Math. Stat. **9** (1938) 60.

[46] LHCb collaboration, L. M. Garcia, L. Henry, B. Kishor, and A. Oyanguren, *Tracking performance for long-lived particles at LHCb*, J. Phys. Conf. Ser. **1525** (2020) 012095, arXiv:1910.06171.

[47] LHCb collaboration, R. Aaij *et al.*, *Search for the radiative $\Xi_b^- \to \Xi^- \gamma$ decay*, JHEP **01** (2022) 069, arXiv:2108.07678.

LHCb collaboration

R. Aaij[38], A.S.W. Abdelmotteleb[57], C. Abellan Beteta[51], F. Abudinén[57], T. Ackernley[61], A. A. Adefisoye[69], B. Adeva[47], M. Adinolfi[55], P. Adlarson[82], C. Agapopoulou[14], C.A. Aidala[84], Z. Ajaltouni[11], S. Akar[66], K. Akiba[38], P. Albicocco[28], J. Albrecht[19,f], F. Alessio[49], M. Alexander[60], Z. Aliouche[63], P. Alvarez Cartelle[56], R. Amalric[16], S. Amato[3], J.L. Amey[55], Y. Amhis[14], L. An[6], L. Anderlini[27], M. Andersson[51], A. Andreianov[44], P. Andreola[51], M. Andreotti[26], D. Andreou[69], A. Anelli[31,o,49], D. Ao[7], F. Archilli[37,u], M. Argenton[26], S. Arguedas Cuendis[9,49], A. Artamonov[44], M. Artuso[69], E. Aslanides[13], R. Ataíde Da Silva[50], M. Atzeni[65], B. Audurier[12], D. Bacher[64], I. Bachiller Perea[10], S. Bachmann[22], M. Bachmayer[50], J.J. Back[57], P. Baladron Rodriguez[47], V. Balagura[15], A. Balboni[26], W. Baldini[26], L. Balzani[19], H. Bao[7], J. Baptista de Souza Leite[61], C. Barbero Pretel[47,12], M. Barbetti[27], I. R. Barbosa[70], R.J. Barlow[63], M. Barnyakov[25], S. Barsuk[14], W. Barter[59], J. Bartz[69], J.M. Basels[17], S. Bashir[40], G. Bassi[35,r], B. Batsukh[5], P. B. Battista[14], A. Bay[50], A. Beck[57], M. Becker[19], F. Bedeschi[35], I.B. Bediaga[2], N. A. Behling[19], S. Belin[47], K. Belous[44], I. Belov[29], I. Belyaev[36], G. Benane[13], G. Bencivenni[28], E. Ben-Haim[16], A. Berezhnoy[44], R. Bernet[51], S. Bernet Andres[45], A. Bertolin[33], C. Betancourt[51], F. Betti[59], J. Bex[56], Ia. Bezshyiko[51], J. Bhom[41], M.S. Bieker[19], N.V. Biesuz[26], P. Billoir[16], A. Biolchini[38], M. Birch[62], F.C.R. Bishop[10], A. Bitadze[63], A. Bizzeti, T. Blake[57], F. Blanc[50], J.E. Blank[19], S. Blusk[69], V. Bocharnikov[44], J.A. Boelhauve[19], O. Boente Garcia[15], T. Boettcher[66], A. Bohare[59], A. Boldyrev[44], C.S. Bolognani[79], R. Bolzonella[26,l], R. B. Bonacci[1], N. Bondar[44], A. Bordelius[49], F. Borgato[33], S. Borghi[63], M. Borsato[31,o], J.T. Borsuk[41], E. Bottalico[61], S.A. Bouchiba[50], M. Bovill[64], T.J.V. Bowcock[61], A. Boyer[49], C. Bozzi[26], J. D. Brandenburg[85], A. Brea Rodriguez[50], N. Breer[19], J. Brodzicka[41], A. Brossa Gonzalo[47,†], J. Brown[61], D. Brundu[32], E. Buchanan[59], L. Buonincontri[33,p], M. Burgos Marcos[79], A.T. Burke[63], C. Burr[49], J.S. Butter[56], J. Buytaert[49], W. Byczynski[49], S. Cadeddu[32], H. Cai[74], A. C. Caillet[16], R. Calabrese[26,l], S. Calderon Ramirez[9], L. Calefice[46], S. Cali[28], M. Calvi[31,o], M. Calvo Gomez[45], P. Camargo Magalhaes[2,z], J. I. Cambon Bouzas[47], P. Campana[28], D.H. Campora Perez[79], A.F. Campoverde Quezada[7], S. Capelli[31], L. Capriotti[26], R. Caravaca-Mora[9], A. Carbone[25,j], L. Carcedo Salgado[47], R. Cardinale[29,m], A. Cardini[32], P. Carniti[31,o], L. Carus[22], A. Casais Vidal[65], R. Caspary[22], G. Casse[61], M. Cattaneo[49], G. Cavallero[26,49], V. Cavallini[26,l], S. Celani[22], S. Cesare[30,n], A.J. Chadwick[61], I. Chahrour[84], M. Charles[16], Ph. Charpentier[49], E. Chatzianagnostou[38], M. Chefdeville[10], C. Chen[13], S. Chen[5], Z. Chen[7], A. Chernov[41], S. Chernyshenko[53], X. Chiotopoulos[79], V. Chobanova[81], M. Chrzaszcz[41], A. Chubykin[44], V. Chulikov[28,36], P. Ciambrone[28], X. Cid Vidal[47], G. Ciezarek[49], P. Cifra[49], P.E.L. Clarke[59], M. Clemencic[49], H.V. Cliff[56], J. Closier[49], C. Cocha Toapaxi[22], V. Coco[49], J. Cogan[13], E. Cogneras[11], L. Cojocariu[43], S. Collaviti[50], P. Collins[49], T. Colombo[49], M. C. Colonna[19], A. Comerma-Montells[46], L. Congedo[24], A. Contu[32], N. Cooke[60], I. Corredoira [47], A. Correia[16], G. Corti[49], J.J. Cottee Meldrum[55], B. Couturier[49], D.C. Craik[51], M. Cruz Torres[2,g], E. Curras Rivera[50], R. Currie[59], C.L. Da Silva[68], S. Dadabaev[44], L. Dai[71], X. Dai[6], E. Dall'Occo[49], J. Dalseno[47], C. D'Ambrosio[49], J. Daniel[11], A. Danilina[44], P. d'Argent[24], G. Darze[3], A. Davidson[57], J.E. Davies[63], O. De Aguiar Francisco[63], C. De Angelis[32,k], F. De Benedetti[49], J. de Boer[38], K. De Bruyn[78], S. De Capua[63], M. De Cian[22], U. De Freitas Carneiro Da Graca[2,a],

E. De Lucia[28], J.M. De Miranda[2], L. De Paula[3], M. De Serio[24,h], P. De Simone[28], F. De Vellis[19], J.A. de Vries[79], F. Debernardis[24], D. Decamp[10], V. Dedu[13], S. Dekkers[1], L. Del Buono[16], B. Delaney[65], H.-P. Dembinski[19], J. Deng[8], V. Denysenko[51], O. Deschamps[11], F. Dettori[32,k], B. Dey[77], P. Di Nezza[28], I. Diachkov[44], S. Didenko[44], S. Ding[69], L. Dittmann[22], V. Dobishuk[53], A. D. Docheva[60], C. Dong[4,b], A.M. Donohoe[23], F. Dordei[32], A.C. dos Reis[2], A. D. Dowling[69], W. Duan[72], P. Duda[80], M.W. Dudek[41], L. Dufour[49], V. Duk[34], P. Durante[49], M. M. Duras[80], J.M. Durham[68], O. D. Durmus[77], A. Dziurda[41], A. Dzyuba[44], S. Easo[58], E. Eckstein[18], U. Egede[1], A. Egorychev[44], V. Egorychev[44], S. Eisenhardt[59], E. Ejopu[63], L. Eklund[82], M. Elashri[66], J. Ellbracht[19], S. Ely[62], A. Ene[43], J. Eschle[69], S. Esen[22], T. Evans[63], F. Fabiano[32], L.N. Falcao[2], Y. Fan[7], B. Fang[7], L. Fantini[34,q,49], M. Faria[50], K. Farmer[59], D. Fazzini[31,o], L. Felkowski[80], M. Feng[5,7], M. Feo[2], A. Fernandez Casani[48], M. Fernandez Gomez[47], A.D. Fernez[67], F. Ferrari[25], F. Ferreira Rodrigues[3], M. Ferrillo[51], M. Ferro-Luzzi[49], S. Filippov[44], R.A. Fini[24], M. Fiorini[26,l], M. Firlej[40], K.L. Fischer[64], D.S. Fitzgerald[84], C. Fitzpatrick[63], T. Fiutowski[40], F. Fleuret[15], M. Fontana[25], L. F. Foreman[63], R. Forty[49], D. Foulds-Holt[56], V. Franco Lima[3], M. Franco Sevilla[67], M. Frank[49], E. Franzoso[26,l], G. Frau[63], C. Frei[49], D.A. Friday[63], J. Fu[7], Q. Führing[19,f,56], Y. Fujii[1], T. Fulghesu[16], E. Gabriel[38], G. Galati[24], M.D. Galati[38], A. Gallas Torreira[47], D. Galli[25,j], S. Gambetta[59], M. Gandelman[3], P. Gandini[30], B. Ganie[63], H. Gao[7], R. Gao[64], T.Q. Gao[56], Y. Gao[8], Y. Gao[6], Y. Gao[8], L.M. Garcia Martin[50], P. Garcia Moreno[46], J. García Pardiñas[49], P. Gardner[67], K. G. Garg[8], L. Garrido[46], C. Gaspar[49], L.L. Gerken[19], E. Gersabeck[63], M. Gersabeck[20], T. Gershon[57], S. G. Ghizzo[29,m], Z. Ghorbanimoghaddam[55], L. Giambastiani[33,p], F. I. Giasemis[16,e], V. Gibson[56], H.K. Giemza[42], A.L. Gilman[64], M. Giovannetti[28], A. Gioventù[46], L. Girardey[63], C. Giugliano[26,l], M.A. Giza[41], E.L. Gkougkousis[62], F.C. Glaser[14,22], V.V. Gligorov[16,49], C. Göbel[70], L. Golinka-Bezshyyko[83], E. Golobardes[45], D. Golubkov[44], A. Golutvin[62,44,49], S. Gomez Fernandez[46], W. Gomulka[40], F. Goncalves Abrantes[64], M. Goncerz[41], G. Gong[4,b], J. A. Gooding[19], I.V. Gorelov[44], C. Gotti[31], E. Govorkova[65], J.P. Grabowski[18], L.A. Granado Cardoso[49], E. Graugés[46], E. Graverini[50,s], L. Grazette[57], G. Graziani, A. T. Grecu[43], L.M. Greeven[38], N.A. Grieser[66], L. Grillo[60], S. Gromov[44], C. Gu[15], M. Guarise[26], L. Guerry[11], V. Guliaeva[44], P. A. Günther[22], A.-K. Guseinov[50], E. Gushchin[44], Y. Guz[6,44,49], T. Gys[49], K. Habermann[18], T. Hadavizadeh[1], C. Hadjivasiliou[67], G. Haefeli[50], C. Haen[49], G. Hallett[57], M.M. Halvorsen[49], P.M. Hamilton[67], J. Hammerich[61], Q. Han[33], X. Han[22,49], S. Hansmann-Menzemer[22], L. Hao[7], N. Harnew[64], T. H. Harris[1], M. Hartmann[14], S. Hashmi[40], J. He[7,c], F. Hemmer[49], C. Henderson[66], R.D.L. Henderson[1,57], A.M. Hennequin[49], K. Hennessy[61], L. Henry[50], J. Herd[62], P. Herrero Gascon[22], J. Heuel[17], A. Hicheur[3], G. Hijano Mendizabal[51], J. Horswill[63], R. Hou[8], Y. Hou[11], N. Howarth[61], J. Hu[72], W. Hu[6], X. Hu[4,b], W. Huang[7], W. Hulsbergen[38], R.J. Hunter[57], M. Hushchyn[44], D. Hutchcroft[61], M. Idzik[40], D. Ilin[44], P. Ilten[66], A. Inglessi[44], A. Iniukhin[44], A. Ishteev[44], K. Ivshin[44], R. Jacobsson[49], H. Jage[17], S.J. Jaimes Elles[75,49,48], S. Jakobsen[49], E. Jans[38], B.K. Jashal[48], A. Jawahery[67], V. Jevtic[19,f], E. Jiang[67], X. Jiang[5,7], Y. Jiang[7], Y. J. Jiang[6], M. John[64], A. John Rubesh Rajan[23], D. Johnson[54], C.R. Jones[56], T.P. Jones[57], S. Joshi[42], B. Jost[49], J. Juan Castella[56], N. Jurik[49], I. Juszczak[41], D. Kaminaris[50], S. Kandybei[52], M. Kane[59], Y. Kang[4,b], C. Kar[11], M. Karacson[49], D. Karpenkov[44], A. Kauniskangas[50], J.W. Kautz[66], M.K. Kazanecki[41], F. Keizer[49], M. Kenzie[56], T. Ketel[38], B. Khanji[69], A. Kharisova[44], S. Kholodenko[35,49], G. Khreich[14], T. Kirn[17], V.S. Kirsebom[31], O. Kitouni[65], S. Klaver[39], N. Kleijne[35,r], K. Klimaszewski[42], M.R. Kmiec[42], S. Koliiev[53], L. Kolk[19], A. Konoplyannikov[44], P. Kopciewicz[49], P. Koppenburg[38], M. Korolev[44], I. Kostiuk[38], O. Kot[53], S. Kotriakhova, A. Kozachuk[44], P. Kravchenko[44], L. Kravchuk[44], M. Kreps[57], P. Krokovny[44], W. Krupa[69], W. Krzemien[42], O. Kshyvanskyi[53], S. Kubis[80], M. Kucharczyk[41], V. Kudryavtsev[44], E. Kulikova[44], A. Kupsc[82], B. K. Kutsenko[13], D. Lacarrere[49], P. Laguarta Gonzalez[46], A. Lai[32], A. Lampis[32], D. Lancierini[56], C. Landesa Gomez[47], J.J. Lane[1], R. Lane[55], G. Lanfranchi[28], C. Langenbruch[22], J. Langer[19], O. Lantwin[44], T. Latham[57], F. Lazzari[35,s,49], C. Lazzeroni[54], R. Le Gac[13], H. Lee[61], R. Lefèvre[11], A. Leflat[44], S. Legotin[44], M. Lehuraux[57], E. Lemos Cid[49], O. Leroy[13], T. Lesiak[41], E. D. Lesser[49], B. Leverington[22], A. Li[4,b], C. Li[13], H. Li[72], K. Li[8], L. Li[63], M. Li[8], P. Li[7], P.-R. Li[73], Q. Li[5,7], S. Li[8], T. Li[5,d], T. Li[72], Y. Li[8], Y. Li[5], Z. Lian[4,b], X. Liang[69], S. Libralon[48], C. Lin[7], T. Lin[58], R. Lindner[49], H. Linton[62], V. Lisovskyi[50], R. Litvinov[32,49], F. L. Liu[1], G. Liu[72], K. Liu[73], S. Liu[5,7], W. Liu[8], Y. Liu[59], Y. Liu[73], Y. L. Liu[62], G. Loachamin Ordonez[70], A. Lobo Salvia[46], A. Loi[32], T. Long[56], J.H. Lopes[3], A. Lopez Huertas[46], S. López Soliño[47], Q. Lu[15], C. Lucarelli[27], D. Lucchesi[33,p], M. Lucio Martinez[79], V. Lukashenko[38,53], Y. Luo[6], A. Lupato[33,i], E. Luppi[26,l], K. Lynch[23], X.-R. Lyu[7], G. M. Ma[4,b], S. Maccolini[19], F. Machefert[14], F. Maciuc[43], B. Mack[69], I. Mackay[64], L. M. Mackey[69], L.R. Madhan Mohan[56], M. J. Madurai[54], A. Maevskiy[44], D. Magdalinski[38], D. Maisuzenko[44], J.J. Malczewski[41], S. Malde[64], L. Malentacca[49], A. Malinin[44], T. Maltsev[44], G. Manca[32,k], G. Mancinelli[13], C. Mancuso[30], R. Manera Escalero[46], F. M. Manganella[37], D. Manuzzi[25], D. Marangotto[30,n], J.F. Marchand[10], R. Marchevski[50], U. Marconi[25], E. Mariani[16], S. Mariani[49], C. Marin Benito[46], J. Marks[22], A.M. Marshall[55], L. Martel[64], G. Martelli[34,q], G. Martellotti[36], L. Martinazzoli[49], M. Martinelli[31,o], D. Martinez Gomez[78], D. Martinez Santos[81], F. Martinez Vidal[48], A. Martorell i Granollers[45], A. Massafferri[2], R. Matev[49], A. Mathad[49], V. Matiunin[44], C. Matteuzzi[69], K.R. Mattioli[15], A. Mauri[62], E. Maurice[15], J. Mauricio[46], P. Mayencourt[50], J. Mazorra de Cos[48], M. Mazurek[42], M. McCann[62], T.H. McGrath[63], N.T. McHugh[60], A. McNab[63], R. McNulty[23], B. Meadows[66], G. Meier[19], D. Melnychuk[42], F. M. Meng[4,b], M. Merk[38,79], A. Merli[50], L. Meyer Garcia[67], D. Miao[5,7], H. Miao[7], M. Mikhasenko[76], D.A. Milanes[75,x], A. Minotti[31,o], E. Minucci[28], T. Miralles[11], B. Mitreska[19], D.S. Mitzel[19], A. Modak[58], L. Moeser[19], R.A. Mohammed[64], R.D. Moise[17], S. Mokhnenko[44], E. F. Molina Cardenas[84], T. Mombächer[49], M. Monk[57,1], S. Monteil[11], A. Morcillo Gomez[47], G. Morello[28], M.J. Morello[35,r], M.P. Morgenthaler[22], J. Moron[40], W. Morren[38], A.B. Morris[49], A.G. Morris[13], R. Mountain[69], H. Mu[4,b], Z. M. Mu[6], E. Muhammad[57], F. Muheim[59], M. Mulder[78], K. Müller[51], F. Muñoz-Rojas[9], R. Murta[62], P. Naik[61], T. Nakada[50], R. Nandakumar[58], T. Nanut[49], I. Nasteva[3], M. Needham[59], N. Neri[30,n], S. Neubert[18], N. Neufeld[49], P. Neustroev[44], J. Nicolini[19], D. Nicotra[79], E.M. Niel[49], N. Nikitin[44], P. Nogarolli[3], P. Nogga[18], C. Normand[55], J. Novoa Fernandez[47], G. Nowak[66], C. Nunez[84], H. N. Nur[60], A. Oblakowska-Mucha[40], V. Obraztsov[44], T. Oeser[17], S. Okamura[26,l], A. Okhotnikov[44], O. Okhrimenko[53], R. Oldeman[32,k], F. Oliva[59], M. Olocco[19], C.J.G. Onderwater[79], R.H. O'Neil[49], D. Osthues[19], J.M. Otalora Goicochea[3], P. Owen[51], A. Oyanguren[48], O. Ozcelik[59], F. Paciolla[35,v], A. Padee[42], K.O. Padeken[18], B. Pagare[57], P.R. Pais[22], T. Pajero[49], A. Palano[24],

M. Palutan[28], X. Pan[4,b], G. Panshin[44], L. Paolucci[57], A. Papanestis[58,49], M. Pappagallo[24,h], L.L. Pappalardo[26,l], C. Pappenheimer[66], C. Parkes[63], D. Parmar[76], B. Passalacqua[26,l], G. Passaleva[27], D. Passaro[35,r,49], A. Pastore[24], M. Patel[62], J. Patoc[64], C. Patrignani[25,j], A. Paul[69], C.J. Pawley[79], A. Pellegrino[38], J. Peng[5,7], M. Pepe Altarelli[28], S. Perazzini[25], D. Pereima[44], H. Pereira Da Costa[68], A. Pereiro Castro[47], P. Perret[11], A. Perrevoort[78], A. Perro[49], M.J. Peters[66], K. Petridis[55], A. Petrolini[29,m], J. P. Pfaller[66], H. Pham[69], L. Pica[35,r], M. Piccini[34], L. Piccolo[32], B. Pietrzyk[10], G. Pietrzyk[14], R. N, Pilato[61], D. Pinci[36], F. Pisani[49], M. Pizzichemi[31,o,49], V. Placinta[43], M. Plo Casasus[47], T. Poeschl[49], F. Polci[16], M. Poli Lener[28], A. Poluektov[13], N. Polukhina[44], I. Polyakov[44], E. Polycarpo[3], S. Ponce[49], D. Popov[7], S. Poslavskii[44], K. Prasanth[59], C. Prouve[81], D. Provenzano[32,k], V. Pugatch[53], G. Punzi[35,s], S. Qasim[51], Q. Q. Qian[6], W. Qian[7], N. Qin[4,b], S. Qu[4,b], R. Quagliani[49], R.I. Rabadan Trejo[57], J.H. Rademacker[55], M. Rama[35], M. Ramírez García[84], V. Ramos De Oliveira[70], M. Ramos Pernas[57], M.S. Rangel[3], F. Ratnikov[44], G. Raven[39], M. Rebollo De Miguel[48], F. Redi[30,i], J. Reich[55], F. Reiss[20], Z. Ren[7], P.K. Resmi[64], M. Ribalda Galvez[46], R. Ribatti[50], G. R. Ricart[15,12], D. Riccardi[35,r], S. Ricciardi[58], K. Richardson[65], M. Richardson-Slipper[59], K. Rinnert[61], P. Robbe[14,49], G. Robertson[60], E. Rodrigues[61], A. Rodriguez Alvarez[46], E. Rodriguez Fernandez[47], J.A. Rodriguez Lopez[75], E. Rodriguez Rodriguez[49], J. Roensch[19], A. Rogachev[44], A. Rogovskiy[58], D.L. Rolf[49], P. Roloff[49], V. Romanovskiy[66], A. Romero Vidal[47], G. Romolini[26], F. Ronchetti[50], T. Rong[6], M. Rotondo[28], S. R. Roy[22], M.S. Rudolph[69], M. Ruiz Diaz[22], R.A. Ruiz Fernandez[47], J. Ruiz Vidal[82,aa], J. Ryzka[40], J. J. Saavedra-Arias[9], J.J. Saborido Silva[47], R. Sadek[15], N. Sagidova[44], D. Sahoo[77], N. Sahoo[54], B. Saitta[32,k], M. Salomoni[31,49,o], I. Sanderswood[48], R. Santacesaria[36], C. Santamarina Rios[47], M. Santimaria[28], L. Santoro [2], E. Santovetti[37], A. Saputi[26,49], D. Saranin[44], A. Sarnatskiy[78], G. Sarpis[59], M. Sarpis[63], C. Satriano[36,t], A. Satta[37], M. Saur[6], D. Savrina[44], H. Sazak[17], F. Sborzacchi[49,28], L.G. Scantlebury Smead[64], A. Scarabotto[19], S. Schael[17], S. Scherl[61], M. Schiller[60], H. Schindler[49], M. Schmelling[21], B. Schmidt[49], S. Schmitt[17], H. Schmitz[18], O. Schneider[50], A. Schopper[49], N. Schulte[19], S. Schulte[50], M.H. Schune[14], R. Schwemmer[49], G. Schwering[17], B. Sciascia[28], A. Sciuccati[49], I. Segal[76], S. Sellam[47], A. Semennikov[44], T. Senger[51], M. Senghi Soares[39], A. Sergi[29,m], N. Serra[51], L. Sestini[33], A. Seuthe[19], Y. Shang[6], D.M. Shangase[84], M. Shapkin[44], R. S. Sharma[69], I. Shchemerov[44], L. Shchutska[50], T. Shears[61], L. Shekhtman[44], Z. Shen[6], S. Sheng[5,7], V. Shevchenko[44], B. Shi[7], Q. Shi[7], Y. Shimizu[14], E. Shmanin[25], R. Shorkin[44], J.D. Shupperd[69], R. Silva Coutinho[69], G. Simi[33,p], S. Simone[24,h], N. Skidmore[57], T. Skwarnicki[69], M.W. Slater[54], J.C. Smallwood[64], E. Smith[65], K. Smith[68], M. Smith[62], A. Snoch[38], L. Soares Lavra[59], M.D. Sokoloff[66], F.J.P. Soler[60], A. Solomin[44,55], A. Solovev[44], I. Solovyev[44], N. S. Sommerfeld[18], R. Song[1], Y. Song[50], Y. Song[4,b], Y. S. Song[6], F.L. Souza De Almeida[69], B. Souza De Paula[3], E. Spadaro Norella[29,m], E. Spedicato[25], J.G. Speer[19], E. Spiridenkov[44], P. Spradlin[60], V. Sriskaran[49], F. Stagni[49], M. Stahl[76], S. Stahl[49], S. Stanislaus[64], M. Stefaniak[85], E.N. Stein[49], O. Steinkamp[51], O. Stenyakin[44], H. Stevens[19], D. Strekalina[44], Y. Su[7], F. Suljik[64], J. Sun[32], L. Sun[74], D. Sundfeld[2], W. Sutcliffe[51], P.N. Swallow[54], K. Swientek[40], F. Swystun[56], A. Szabelski[42], T. Szumlak[40], Y. Tan[4,b], Y. Tang[74], M.D. Tat[22], A. Terentev[44], F. Terzuoli[35,v,49], F. Teubert[49], E. Thomas[49], D.J.D. Thompson[54], H. Tilquin[62], V. Tisserand[11],

S. T'Jampens[10], M. Tobin[5,49], L. Tomassetti[26,l], G. Tonani[30,n], X. Tong[6], T. Tork[30], D. Torres Machado[2], L. Toscano[19], D.Y. Tou[4,b], C. Trippl[45], G. Tuci[22], N. Tuning[38], L.H. Uecker[22], A. Ukleja[40], D.J. Unverzagt[22], B. Urbach[59], A. Usachov[39], A. Ustyuzhanin[44], U. Uwer[22], V. Vagnoni[25], V. Valcarce Cadenas[47], G. Valenti[25], N. Valls Canudas[49], J. van Eldik[49], H. Van Hecke[68], E. van Herwijnen[62], C.B. Van Hulse[47,y], R. Van Laak[50], M. van Veghel[38], G. Vasquez[51], R. Vazquez Gomez[46], P. Vazquez Regueiro[47], C. Vázquez Sierra[47], S. Vecchi[26], J.J. Velthuis[55], M. Veltri[27,w], A. Venkateswaran[50], M. Verdoglia[32], M. Vesterinen[57], D. Vico Benet[64], P. Vidrier Villalba[46], M. Vieites Diaz[47], X. Vilasis-Cardona[45], E. Vilella Figueras[61], A. Villa[25], P. Vincent[16], F.C. Volle[54], D. vom Bruch[13], N. Voropaev[44], K. Vos[79], C. Vrahas[59], J. Wagner[19], J. Walsh[35], E.J. Walton[1,57], G. Wan[6], C. Wang[22], G. Wang[8], J. Wang[6], J. Wang[5], J. Wang[4,b], J. Wang[74], M. Wang[49], N. W. Wang[7], R. Wang[55], X. Wang[8], X. Wang[72], X. W. Wang[62], Y. Wang[6], Z. Wang[14], Z. Wang[4,b], Z. Wang[30], J.A. Ward[57,1], M. Waterlaat[49], N.K. Watson[54], D. Websdale[62], Y. Wei[6], J. Wendel[81], B.D.C. Westhenry[55], C. White[56], M. Whitehead[60], E. Whiter[54], A.R. Wiederhold[63], D. Wiedner[19], G. Wilkinson[64], M.K. Wilkinson[66], M. Williams[65], M. J. Williams[49], M.R.J. Williams[59], R. Williams[56], Z. Williams[55], F.F. Wilson[58], M. Winn[12], W. Wislicki[42], M. Witek[41], L. Witola[22], G. Wormser[14], S.A. Wotton[56], H. Wu[69], J. Wu[8], X. Wu[74], Y. Wu[6], Z. Wu[7], K. Wyllie[49], S. Xian[72], Z. Xiang[5], Y. Xie[8], T. X. Xing[30], A. Xu[35], L. Xu[4,b], L. Xu[4,b], M. Xu[57], Z. Xu[49], Z. Xu[7], Z. Xu[5], K. Yang[62], S. Yang[7], X. Yang[6], Y. Yang[29,m], Z. Yang[6], V. Yeroshenko[14], H. Yeung[63], H. Yin[8], X. Yin[7], C. Y. Yu[6], J. Yu[71], X. Yuan[5], Y Yuan[5,7], E. Zaffaroni[50], M. Zavertyaev[21], M. Zdybal[41], F. Zenesini[25], C. Zeng[5,7], M. Zeng[4,b], C. Zhang[6], D. Zhang[8], J. Zhang[7], L. Zhang[4,b], S. Zhang[71], S. Zhang[64], Y. Zhang[6], Y. Z. Zhang[4,b], Z. Zhang[4,b], Y. Zhao[22], A. Zhelezov[22], S. Z. Zheng[6], X. Z. Zheng[4,b], Y. Zheng[7], T. Zhou[6], X. Zhou[8], Y. Zhou[7], V. Zhovkovska[57], L. Z. Zhu[7], X. Zhu[4,b], X. Zhu[8], V. Zhukov[17], J. Zhuo[48], Q. Zou[5,7], D. Zuliani[33,p], G. Zunica[50].

[1] *School of Physics and Astronomy, Monash University, Melbourne, Australia*
[2] *Centro Brasileiro de Pesquisas Físicas (CBPF), Rio de Janeiro, Brazil*
[3] *Universidade Federal do Rio de Janeiro (UFRJ), Rio de Janeiro, Brazil*
[4] *Department of Engineering Physics, Tsinghua University, Beijing, China, Beijing, China*
[5] *Institute Of High Energy Physics (IHEP), Beijing, China*
[6] *School of Physics State Key Laboratory of Nuclear Physics and Technology, Peking University, Beijing, China*
[7] *University of Chinese Academy of Sciences, Beijing, China*
[8] *Institute of Particle Physics, Central China Normal University, Wuhan, Hubei, China*
[9] *Consejo Nacional de Rectores (CONARE), San Jose, Costa Rica*
[10] *Université Savoie Mont Blanc, CNRS, IN2P3-LAPP, Annecy, France*
[11] *Université Clermont Auvergne, CNRS/IN2P3, LPC, Clermont-Ferrand, France*
[12] *Université Paris-Saclay, Centre d¿Etudes de Saclay (CEA), IRFU, Saclay, France, Gif-Sur-Yvette, France*
[13] *Aix Marseille Univ, CNRS/IN2P3, CPPM, Marseille, France*
[14] *Université Paris-Saclay, CNRS/IN2P3, IJCLab, Orsay, France*
[15] *Laboratoire Leprince-Ringuet, CNRS/IN2P3, Ecole Polytechnique, Institut Polytechnique de Paris, Palaiseau, France*
[16] *LPNHE, Sorbonne Université, Paris Diderot Sorbonne Paris Cité, CNRS/IN2P3, Paris, France*
[17] *I. Physikalisches Institut, RWTH Aachen University, Aachen, Germany*
[18] *Universität Bonn - Helmholtz-Institut für Strahlen und Kernphysik, Bonn, Germany*
[19] *Fakultät Physik, Technische Universität Dortmund, Dortmund, Germany*
[20] *Physikalisches Institut, Albert-Ludwigs-Universität Freiburg, Freiburg, Germany*

[21]*Max-Planck-Institut für Kernphysik (MPIK), Heidelberg, Germany*
[22]*Physikalisches Institut, Ruprecht-Karls-Universität Heidelberg, Heidelberg, Germany*
[23]*School of Physics, University College Dublin, Dublin, Ireland*
[24]*INFN Sezione di Bari, Bari, Italy*
[25]*INFN Sezione di Bologna, Bologna, Italy*
[26]*INFN Sezione di Ferrara, Ferrara, Italy*
[27]*INFN Sezione di Firenze, Firenze, Italy*
[28]*INFN Laboratori Nazionali di Frascati, Frascati, Italy*
[29]*INFN Sezione di Genova, Genova, Italy*
[30]*INFN Sezione di Milano, Milano, Italy*
[31]*INFN Sezione di Milano-Bicocca, Milano, Italy*
[32]*INFN Sezione di Cagliari, Monserrato, Italy*
[33]*INFN Sezione di Padova, Padova, Italy*
[34]*INFN Sezione di Perugia, Perugia, Italy*
[35]*INFN Sezione di Pisa, Pisa, Italy*
[36]*INFN Sezione di Roma La Sapienza, Roma, Italy*
[37]*INFN Sezione di Roma Tor Vergata, Roma, Italy*
[38]*Nikhef National Institute for Subatomic Physics, Amsterdam, Netherlands*
[39]*Nikhef National Institute for Subatomic Physics and VU University Amsterdam, Amsterdam, Netherlands*
[40]*AGH - University of Krakow, Faculty of Physics and Applied Computer Science, Kraków, Poland*
[41]*Henryk Niewodniczanski Institute of Nuclear Physics Polish Academy of Sciences, Kraków, Poland*
[42]*National Center for Nuclear Research (NCBJ), Warsaw, Poland*
[43]*Horia Hulubei National Institute of Physics and Nuclear Engineering, Bucharest-Magurele, Romania*
[44]*Affiliated with an institute covered by a cooperation agreement with CERN*
[45]*DS4DS, La Salle, Universitat Ramon Llull, Barcelona, Spain*
[46]*ICCUB, Universitat de Barcelona, Barcelona, Spain*
[47]*Instituto Galego de Física de Altas Enerxías (IGFAE), Universidade de Santiago de Compostela, Santiago de Compostela, Spain*
[48]*Instituto de Fisica Corpuscular, Centro Mixto Universidad de Valencia - CSIC, Valencia, Spain*
[49]*European Organization for Nuclear Research (CERN), Geneva, Switzerland*
[50]*Institute of Physics, Ecole Polytechnique Fédérale de Lausanne (EPFL), Lausanne, Switzerland*
[51]*Physik-Institut, Universität Zürich, Zürich, Switzerland*
[52]*NSC Kharkiv Institute of Physics and Technology (NSC KIPT), Kharkiv, Ukraine*
[53]*Institute for Nuclear Research of the National Academy of Sciences (KINR), Kyiv, Ukraine*
[54]*School of Physics and Astronomy, University of Birmingham, Birmingham, United Kingdom*
[55]*H.H. Wills Physics Laboratory, University of Bristol, Bristol, United Kingdom*
[56]*Cavendish Laboratory, University of Cambridge, Cambridge, United Kingdom*
[57]*Department of Physics, University of Warwick, Coventry, United Kingdom*
[58]*STFC Rutherford Appleton Laboratory, Didcot, United Kingdom*
[59]*School of Physics and Astronomy, University of Edinburgh, Edinburgh, United Kingdom*
[60]*School of Physics and Astronomy, University of Glasgow, Glasgow, United Kingdom*
[61]*Oliver Lodge Laboratory, University of Liverpool, Liverpool, United Kingdom*
[62]*Imperial College London, London, United Kingdom*
[63]*Department of Physics and Astronomy, University of Manchester, Manchester, United Kingdom*
[64]*Department of Physics, University of Oxford, Oxford, United Kingdom*
[65]*Massachusetts Institute of Technology, Cambridge, MA, United States*
[66]*University of Cincinnati, Cincinnati, OH, United States*
[67]*University of Maryland, College Park, MD, United States*
[68]*Los Alamos National Laboratory (LANL), Los Alamos, NM, United States*
[69]*Syracuse University, Syracuse, NY, United States*
[70]*Pontifícia Universidade Católica do Rio de Janeiro (PUC-Rio), Rio de Janeiro, Brazil, associated to* [3]
[71]*School of Physics and Electronics, Hunan University, Changsha City, China, associated to* [8]
[72]*Guangdong Provincial Key Laboratory of Nuclear Science, Guangdong-Hong Kong Joint Laboratory of Quantum Matter, Institute of Quantum Matter, South China Normal University, Guangzhou, China, associated to* [4]

[73]Lanzhou University, Lanzhou, China, associated to [5]
[74]School of Physics and Technology, Wuhan University, Wuhan, China, associated to [4]
[75]Departamento de Fisica , Universidad Nacional de Colombia, Bogota, Colombia, associated to [16]
[76]Ruhr Universitaet Bochum, Fakultaet f. Physik und Astronomie, Bochum, Germany, associated to [19]
[77]Eotvos Lorand University, Budapest, Hungary, associated to [49]
[78]Van Swinderen Institute, University of Groningen, Groningen, Netherlands, associated to [38]
[79]Universiteit Maastricht, Maastricht, Netherlands, associated to [38]
[80]Tadeusz Kosciuszko Cracow University of Technology, Cracow, Poland, associated to [41]
[81]Universidade da Coruña, A Coruña, Spain, associated to [45]
[82]Department of Physics and Astronomy, Uppsala University, Uppsala, Sweden, associated to [60]
[83]Taras Schevchenko University of Kyiv, Faculty of Physics, Kyiv, Ukraine, associated to [14]
[84]University of Michigan, Ann Arbor, MI, United States, associated to [69]
[85]Ohio State University, Columbus, United States, associated to [68]

[a]Centro Federal de Educacão Tecnológica Celso Suckow da Fonseca, Rio De Janeiro, Brazil
[b]Center for High Energy Physics, Tsinghua University, Beijing, China
[c]Hangzhou Institute for Advanced Study, UCAS, Hangzhou, China
[d]School of Physics and Electronics, Henan University , Kaifeng, China
[e]LIP6, Sorbonne Université, Paris, France
[f]Lamarr Institute for Machine Learning and Artificial Intelligence, Dortmund, Germany
[g]Universidad Nacional Autónoma de Honduras, Tegucigalpa, Honduras
[h]Università di Bari, Bari, Italy
[i]Università di Bergamo, Bergamo, Italy
[j]Università di Bologna, Bologna, Italy
[k]Università di Cagliari, Cagliari, Italy
[l]Università di Ferrara, Ferrara, Italy
[m]Università di Genova, Genova, Italy
[n]Università degli Studi di Milano, Milano, Italy
[o]Università degli Studi di Milano-Bicocca, Milano, Italy
[p]Università di Padova, Padova, Italy
[q]Università di Perugia, Perugia, Italy
[r]Scuola Normale Superiore, Pisa, Italy
[s]Università di Pisa, Pisa, Italy
[t]Università della Basilicata, Potenza, Italy
[u]Università di Roma Tor Vergata, Roma, Italy
[v]Università di Siena, Siena, Italy
[w]Università di Urbino, Urbino, Italy
[x]Universidad de Ingeniería y Tecnología (UTEC), Lima, Peru
[y]Universidad de Alcalá, Alcalá de Henares , Spain
[z]Facultad de Ciencias Fisicas, Madrid, Spain
[aa]Department of Physics/Division of Particle Physics, Lund, Sweden

[†]Deceased